Int. J. Electrochem. Sci., 10 **(2015)** 259 - 271

International Journal of
ELECTROCHEMICAL
SCIENCE
www.electrochemsci.org

2, 10-dimethylacridin-9(10H)-one as New Synthesized Corrosion Inhibitor for C38 Steel in 0.5 M H_2SO_4

R. Salghi[1,*], *D. Ben Hmamou*[1], *Eno E. Ebenso*[2,*], *O. Benali*[3], *A. Zarrouk*[4], *B. Hammouti*[4]

[1] Equipe de Génie de l'Environnement et Biotechnologie, ENSA, Université Ibn Zohr, BP1136 Agadir, Morocco
[2] Material Science Innovation & Modelling (MaSIM) Research Focus Area, Faculty of Agriculture, Science and Technology, North-West University (Mafikeng Campus), Private Bag X2046, Mmabatho 2735, South Africa
[3] Départment de Biologie, Faculté des sciences et de la technologie, Université Dr. Tahar Moulay – Saïda- Algeria
[4] LCAE-URAC18, Faculté des Sciences, Université Mohammed 1er, Oujda, Morocco.
[*]E-mail: r.salghi@uiz.ac.ma; Eno.Ebenso@nwu.ac.za

Received: 19 September 2014 / *Accepted:* 4 November 2014 / *Published:* 17 November 2014

The corrosion inhibition of C38 steel in 0.5 M H_2SO_4 solution by 2,10-dimethylacridin-9(10H)-one (DMA) has been studied using electrochemical polarization , electrochemical impedance spectroscopy (EIS) and weight loss methods. The corrosion inhibition efficiency measured by all the three techniques was in good agreement with each other. The results showed that DMA is a very good inhibitor for C38 steel in acidic media. The inhibition efficiency increases with increasing inhibitor concentration and with increasing temperature. It acts as a mixed-type inhibitor. Thermodynamic and activation parameters obtained from the study are discussed. Adsorption of DMA was found to follow the Langmuir's adsorption isotherm and chemisorption mechanism is proposed.

Keywords: corrosion inhibitors, 2,10-dimethylacridin-9(10H)-one, C38 steel, sulphuric acid, thermodynamic functions, adsorption process.

1. INTRODUCTION

The use of inhibitors is one of the most practical methods for protection against corrosion, especially in acidic solution [1]. Many organic compounds are widely used as acid inhibitors in industrial operations, such as pickling, cleaning, acidization of oil wells, to protect metals and alloys[2-3]. The organic substances containing mainly oxygen, sulphur, nitrogen atoms, and multiple bonds in the molecules that facilitate the adsorption on the metal surface are strongly polar [4-9]. The polar unit

is regarded as the reaction center for the adsorption process. Thus, polar organic compounds are adsorbed on the metal surface, forming a charge transfer complex bond between their polar atoms and the metal. The size, orientation, shape and electric charge on the molecule determine the degree of adsorption and hence the effectiveness of the inhibitor [10-16]. View the wide applications of acridine derivatives in various fields of biology, such as photodynamic therapy [13], anti-cancer [14]… in one hand and the encouraging results in inhibition corrosion of metals [15-16] on the other hand; it is interesting to find an easy way to new aciridine molecules. In the present work, the efficiency of a new synthesized organic compound 2,10-dimethylacridin-9(10H)-one (DMA) as inhibitor for the corrosion of C38 steel in 0.5 M sulphuric acid is reported using weight loss, electrochemical impedance spectroscopy (EIS) and Tafel polarization methods. The structure of synthesized organic compound 2,10-dimethylacridin-9(10H)-one (DMA) is shown in Figure 1.

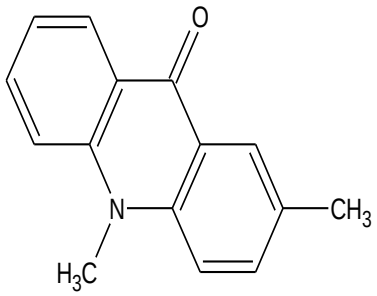

Figure 1. Molecular structure of 2,10-dimethylacridin-9(10*H*)-one (**DMA)**

2. MATERIALS AND METHODS

2.1. Weight loss measurements

The steel used in this study is a carbon steel (Euronorm: C35E carbon steel and US specification: SAE 1035) with a chemical composition (in wt%) of 0.370 % C, 0.230 % Si, 0.680 % Mn, 0.016 % S, 0.077 % Cr, 0.011 % Ti, 0.059 % Ni, 0.009 % Co, 0.160 % Cu and the remainder iron (Fe). Coupons were cut into 2 × 2 × 0.08 cm^3 dimensions are used for weight loss measurements. Prior to all measurements, the exposed area was mechanically abraded with 180, 320, 800, 1200 grades of emery papers. The specimens are washed thoroughly with bidistilled water, degreased and dried with ethanol. Gravimetric measurements are carried out in a double walled glass cell equipped with a thermostated cooling condenser. The solution volume is 80 cm^3. The immersion time for the weight loss is 6 h at 298 K.

2.2. Electrochemical tests

The electrochemical study was carried out using a potentiostat PGZ100 piloted by Voltamaster software. This potentiostat is connected to a cell with three electrode thermostats with double wall (Tacussel Standard CEC/TH). A saturated calomel electrode (SCE) and platinum electrode were used

as reference and auxiliary electrodes, respectively. The material used for constructing the working electrode was the same used for gravimetric measurements. The surface area exposed to the electrolyte is 0.04 cm^2. Potentiodynamic polarization curves were plotted at a polarization scan rate of 0.5 mV/s. Before all experiments, the potential was stabilized at free potential during 30 min. The polarization curves are obtained from −800 mV to −200 mV at 298 K. The solution test is there after de-aerated by bubbling nitrogen. Gas bubbling is maintained prior and through the experiments. In order to investigate the effects of temperature and immersion time on the inhibitor performance, some test were carried out in a temperature range 298–328 K. The electrochemical impedance spectroscopy (EIS) measurements are carried out with the electrochemical system (Tacussel), which included a digital potentiostat model Voltalab PGZ100 computer at E_{corr} after immersion in solution with bubbling. After the determination of steady-state current at a corrosion potential, sine wave voltage (10 mV) peak to peak, at frequencies between 100 kHz and 10 mHz are superimposed on the rest potential. Computer programs automatically controlled the measurements performed at rest potentials after 0.5 hour of exposure at 298 K. The impedance diagrams are given in the Nyquist representation. Experiments are repeated three times to ensure the reproducibility.

3. RESULTS AND DISCUSSION

3.1. Effect of concentration

3.1.1. Weight loss, corrosion rates and inhibition efficiency

Table 1. Effect of **DMA** concentration on corrosion data of C38 steel in 0.5 M H_2SO_4

Conc. (M)	W_{corr} (mg. cm^{-2})	IE_w (%)
Blank	1.790	----
10^{-6}	0.5615	68.63
10^{-5}	0.4331	75.80
10^{-4}	0.3504	80.42
10^{-3}	0.1145	93.60

Values of the inhibition efficiency and corrosion rate obtained from the weight loss measurements of C38 steel for different concentrations of DMA in 0.5 M H_2SO_4 at 298 K after 6 hours of immersion are given in table 1.

The corrosion rate (W_{corr}) of carbon steel coupons in 0.5M H_2SO_4 solution at different concentrations of DMA was determined after 6 h of immersion time at 298 K and calculated using the following equation:

$$W_{corr} = \frac{m}{S.t} \quad (1)$$

Where m is the weight loss of C38 steel sheets, S the total area of one C38 steel sheets, and t is immersion time.

Inhibition efficiency IE_w (%) was calculated as follows:

$$IE_w\ (\%) = \frac{W_{0\ corr} - W_{corr}}{W_{corr}} \times 100 \qquad (2)$$

where $W_{0\,corr}$ and W_{corr} are the corrosion rates of C38 steel due to the dissolution in 0.5 M H_2SO_4 in the absence and presence of different concentrations of inhibitor, respectively.

From this table we can see that the inhibition efficiency increases with the increasing inhibitor concentration. From the results one observes that the optimum concentration of inhibitor required to achieve the efficiency was found to be 10^{-3} M (IE_w=93.60 %).

3.1.2. Polarization curves

Figure 2 shows the polarization curves of C38 steel in 0.5 M H_2SO_4 and in the presence of different concentrations (10^{-6} to 10^{-3} M) of DMA. With the increase of DMA concentrations, both anodic and cathodic currents were inhibited. This result shows that the addition of DMA inhibitor reduces anodic dissolution and also retards the hydrogen evolution reaction.

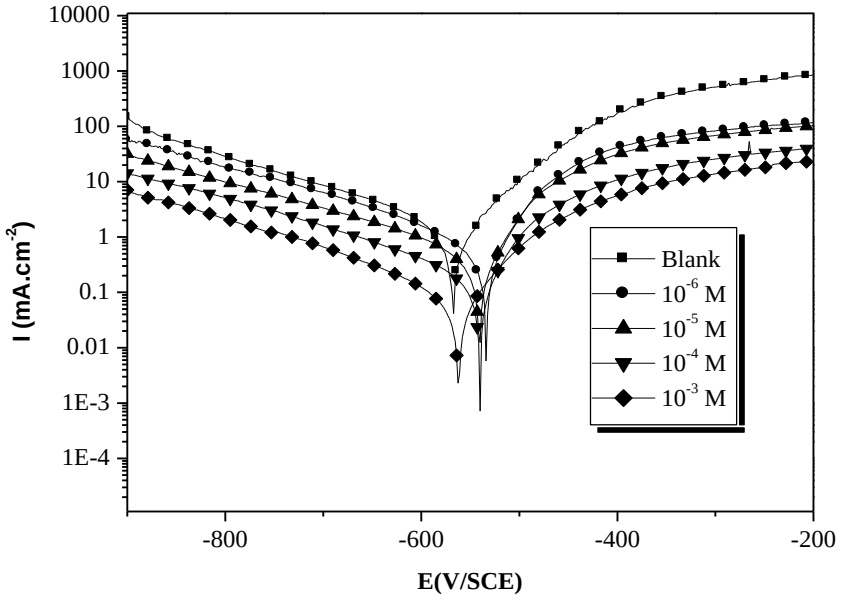

Figure 2. Potentiodynamic polarization curves of C38 steel in 0.5M H_2SO_4 in the presence of different concentrations of DMA.

The inhibition efficiencies were calculated from I_{corr} values according to following equation:

$$IE_{Icorr}(\%) = \frac{I_{0\,corr} - I_{corr}}{I_{0\,corr}} \times 100 \quad (3)$$

Where $I_{0\,corr}$ and I_{corr} are the corrosion current densities in the absence and the presence of the inhibitor.

Table 2 gives the values of corrosion kinetic parameters as the corrosion potential E_{corr} , corrosion current density I_{corr} , cathodic Tafel slope (b_c), and inhibition efficiency (IE_{Icorr}) for the corrosion of C38 steel in 0.5M H_2SO_4 with different concentrations of DMA. The corrosion current densities were estimated by Tafel extrapolation of the cathodic curves to the open circuit corrosion potentials.

Table 2. Electrochemical parameters of C38 steel at various concentrations of DMA in 0.5M H_2SO_4 and corresponding inhibition efficiency.

Conc. (M)	E_{corr} (mV/SCE)	I_{corr} (mA/cm^2)	$-b_c$ (mV/dec)	b_a (mV/dec)	IE_{Icorr} (%)
Blank	-567	2.55	186	77	----
10^{-6}	-534	0.80	183	43	68.62
10^{-5}	-536	0.57	178	52	77.65
10^{-4}	-540	0.32	181	93	87.45
10^{-3}	-559	0.20	179	144	92.16

These results revealed that the corrosion current density (I_{corr}) decreased remarkably with the increasing inhibitor concentrations, leading to the increase of inhibition efficiency.

A compound is usually classified as an anodic or a cathodic type inhibitor when the change in E_{corr} value is larger than 85 mV [17-18]. Since the small displacement of the corrosion potential was about 18 mV (Table 2) after the addition of the DMA, suggesting that the inhibitor acted as a mixed-type inhibitor. The values of the cathodic Tafel slopes, b_c, were found to vary a range of 186-178 mV/dec. Therefore, the cathodic slope value was found to remain constant with increasing concentration of DMA in 0.5M H_2SO_4. Thus, the presence of the inhibitor does not affect the cathodic slopes (b_c). This indicates that addition of DMA does not modify the mechanism of the proton discharge reaction. The values of inhibition efficiency (IE_{Icorr} %) increase with inhibitor concentration reaching a maximum value (92.16 %) at 10^{-3} M.

3.1.3. Electrochemical impedance spectroscopy measurements:

Nyquist plots of C38 steel in 0.5 M H_2SO_4 in the presence and absence of additive are given in Figure 3. These curves were obtained after 0.5 h of immersion in the corresponding solution.

All the plots display a single capacitive loop. Impedance parameters derived from the Nyquist plots, percent inhibition efficiencies, EI_{Rt} (%) and the equivalent circuit diagram are given in Table 3 and Figure 4, respectively.

The values of R_t were given by subtracting the high frequency impedance from the low frequency one as follow [19]:

$$R_t = Z_{re}(\text{at low frequency}) - Z_{re}(\text{at high frequency}) \quad (4)$$

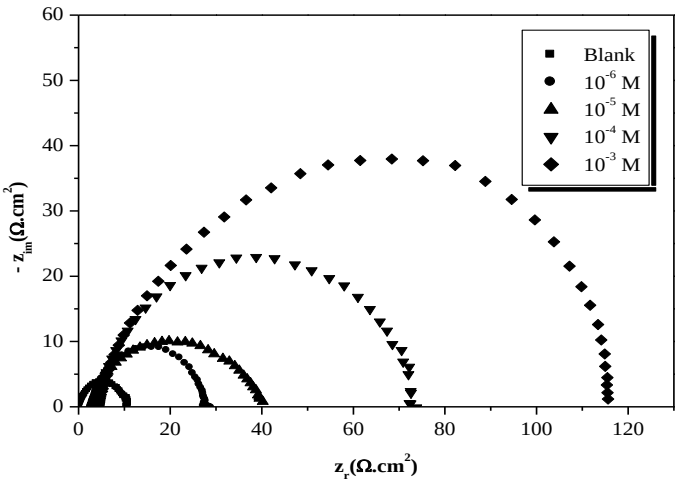

Figure 3. Nyquist diagrams for C38 steel electrode with and without DMA at E_{corr} after 30min of immersion.

The values of electrochemical double layer capacitance, C_{dl} were calculated at the frequency f_{max}, at which the imaginary component of the impedance is maximal ($-Z_{max}$) by the following equation [15]:

$$C_{dl} = \frac{1}{2\pi f_{max} R_t} \quad (5)$$

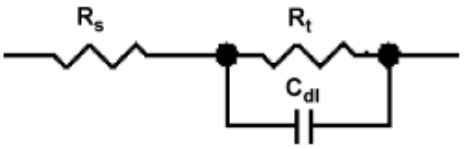

Figure 4. The electrochemical equivalent circuit used to fit the impedance spectra.

The percent inhibition efficiency (IE_{Rt}) is calculated by charge transfer resistance obtained from Nyquist plots, according to the equation:

$$IE_{Rt}(\%) = \frac{R_t - R_t^0}{R_t} \times 100 \quad (6)$$

where R_t^0 and R_t are the charge transfer resistance values without and with inhibitor, respectively.

Table 3. Electrochemical Impedance parameters for corrosion of C38 steel in acid medium at various contents of DMA

Conc. (M)	R_t ($\Omega.cm^2$)	C_{dl} ($\mu F/cm^2$)	IE_{Rt} (%)
Blank	10.58	215.09	-----
10^{-6}	38.50	41.27	72.51
10^{-5}	40.00	39.65	73.55
10^{-4}	75.32	21.72	85.95
10^{-3}	127.2	17.11	91.68

As can be seen from this table the increase in resistance in the presence of DMA, compared to H_2SO_4, alone is related to the corrosion inhibition effect of the molecules. The value of C_{dl} decreases in the presence of this inhibitor. The decrease in C_{dl}, which can result from a decrease in local dielectric constant and/or an increase in the thickness of the electric double layer [16, 20], suggested that DMA molecules function by adsorption at the metal/solution interface. Thus, the decrease in C_{dl} values and the increase in R_t values and consequently of inhibition efficiency may be due to the gradual replacement of water molecules by the adsorption of the DMA molecules on the metal surface, decreasing the extent of dissolution reaction [21-22].

The results obtained by this method are in good agreement with the values of inhibitor efficiency obtained from weight loss and polarization measurements.

3.2. Adsorption isotherm

It is known that the adsorption isotherms are very important for the understanding of the mechanism of corrosion inhibition. Assuming a direct relationship between inhibition efficiency and surface coverage, θ, of the inhibitor, electrochemical impedance spectroscopy data were used to evaluate the surface coverage values, described in Eq. (7):

$$\theta = \frac{R_t - R_t^0}{R_t} \qquad (7)$$

where R_t^0 and R_t are the charge transfer resistance values without and with inhibitor, respectively.

The surface coverage values (θ) were tested graphically to allow fitting of a suitable adsorption isotherm. The plot of C/θ vs. C (Fig. 6) yielded straight line with slope equal to 1.09, clearly proving that the adsorption of the DMA from 0.5 M H_2SO_4 solution on the C38 steel obeys the Langmuir adsorption isotherm where,

$$\frac{C}{\theta} = \frac{1}{K} + C \qquad (8)$$

with

$$K = \frac{1}{55,5}\exp(-\frac{\Delta G^{0}{}_{ads}}{RT}) \quad (9)$$

where K is the equilibrium constant for the adsorption process, C is the concentration of the inhibitor and θ is the surface coverage.

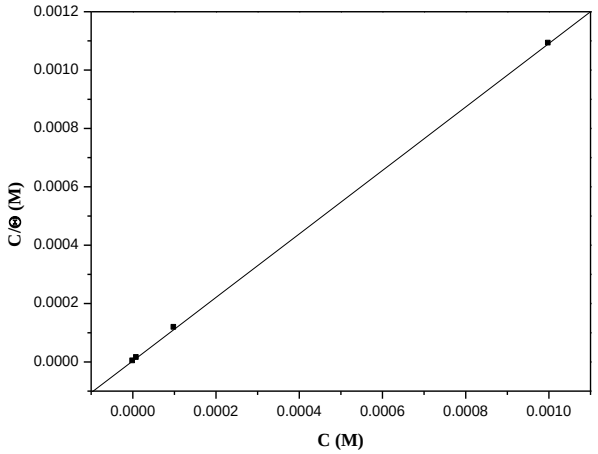

Figure 5. Curves fitting of the corrosion data of C38 steel in the presence of inhibitor to Langmuir isotherm.

The value of equilibrium adsorption constant obtained from this isotherm is about 2.95 x 10^5 M^{-1}, suggesting a chemically adsorbed film [23]. Moreover, the largest negative values of ΔG_{ads}, i.e. -41.13 kJ/mol for DMA, indicate that this inhibitor is strongly adsorbed onto the C38 steel surface. It is well known that values of $-\Delta G_{ads}$ of the order of 20 kJ/mol or lower indicate a physisorption; those of order of 40 kJ/ mol or higher involve charge sharing or a transfer from the inhibitor molecules to the metal surface to form a co-ordinate type of bond [24-25]. We can note that a plausible mechanism of corrosion inhibition of C38 steel in 0.5 M H_2SO_4 by the compounds under study may be deduced on the basis of adsorption. In acidic solutions, these inhibitors can exist as cationic species which may be adsorbed on the cathodic sites of the C38 steel and reduce the evolution of hydrogen. The protonated inhibitor can also be adsorbed on the metal surface on specifically adsorbed sulphate ions, which act as a bridge between the metal surface and the electrolyte. Moreover, the adsorption of these compounds on anodic sites through lone pairs of electrons of nitrogen and oxygen atoms and through π-electrons of $C = O$ and phenyl groups will then reduce the anodic dissolution of C38 steel [6, 26].

3.3. Effect of temperature:

In order to study the effect of temperature on corrosion inhibition of C38 steel in the acid reaction and to determine the activation energy of the corrosion process, the polarization curves were done at various temperatures (298-328 K) in the absence and in the presence of DMA at optimal concentration (Figures 6 and 7).

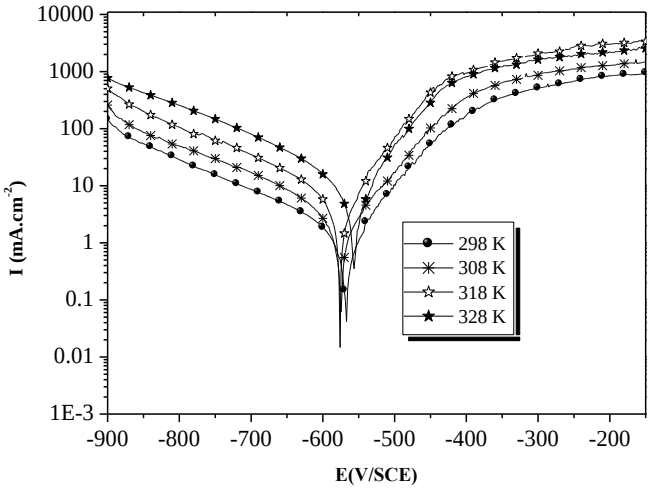

Figure 6. Potentiodynamic polarisation curves of C38 steel in 0.5 M H_2SO_4 at different temperatures

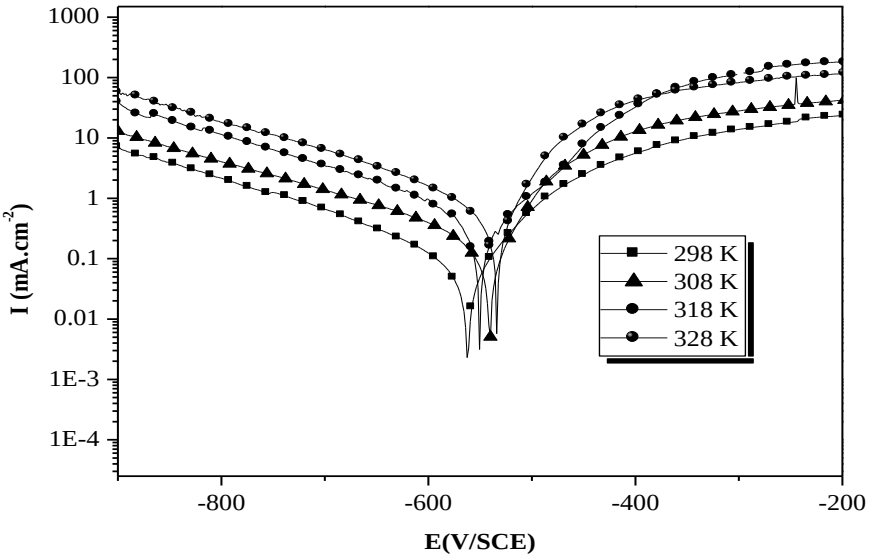

Figure 7. Potentiodynamic polarization curves of C38 steel in 0.5M H_2SO_4 in the presence of 10^{-3} M of DMA inhibitor at different temperatures.

The corresponding results are given in table 4. We note that In the studied temperature range (298 -328 K), the corrosion current density increases with increasing temperature both in uninhibited and inhibited solutions and the values of the inhibition efficiency of DMA are nearly constant. The corrosion current density of steel increases more rapidly with temperature in the absence of the inhibitor, these results confirm that DMA acts as an efficient inhibitor in the range of temperature studied. The DMA inhibitor efficiency was temperature independent.

Table 4. Various corrosion parameters for C38 steel in 0.5 M H_2SO_4 in absence and presence of optimum concentration of DMA at different temperatures.

Temperature (K)	E_{corr} (mV/SCE)	I_{corr} (mA/cm^2)	$-b_c$ (mV/dec)	b_a (mV/dec)	IE_{Icorr} (%)
298	-454	2.55	186	77	----
308	-460	3.78	181	65	----
318	-462	7.92	176	54	----
328	-445	15.80	172	51	----
298	-559	0.20	183	144	92.00
308	-538	0.26	181	82	93.11
318	-551	0.57	185	64	92.79
328	-533	0.94	178	42	94.05

The activation parameters for the corrosion process were calculated from Arrhenius type plot according to the following:

$$\log I = -\frac{E_a}{2.303\,R\,T} + \log A \qquad (10)$$

where E_a is the apparent activation energy, T is the absolute temperature, k is the Arrhenius pre-exponential constant and R is the universal gas constant.

And an alternative formulation of Arrhenius equation is:

$$I_{corr} = \frac{RT}{Nh}\exp\left(\frac{\Delta S_a^0}{R}\right)\exp\left(-\frac{\Delta H_a^0}{RT}\right) \qquad (11)$$

where h is Planck's constant, N is Avogadro's number, ΔS_a is the entropy of activation and ΔH_a is the enthalpy of activation.

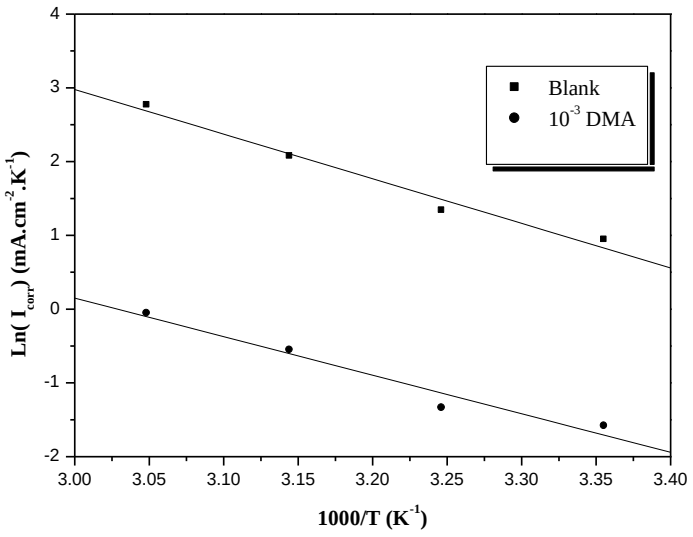

Figure 8. Arrhenius plots of steel in 0.5 M H_2SO_4 with and without 10^{-3} M of DMA

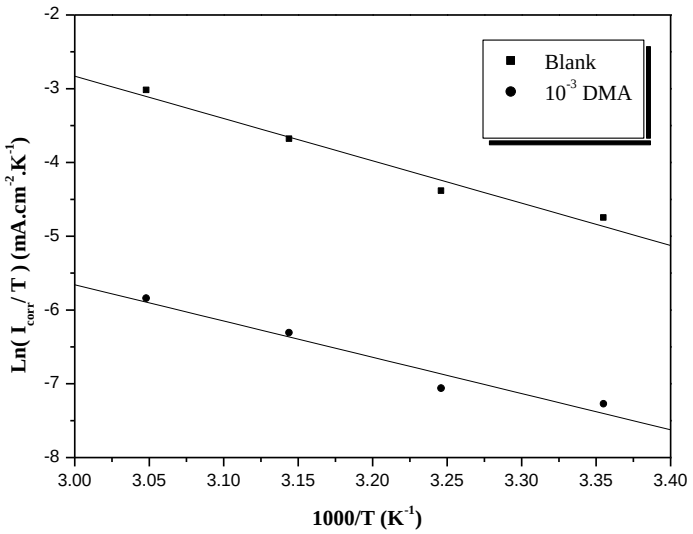

Figure 9. Transition state plots of Ln (I_{corr}/T) versus 10^3/T for blank and 1M H_2SO_4 + 10^{-3} M DMA

The variation of logarithm of the corrosion rate of C38 steel (log I) in sulphuric acid containing the optimal concentration of DMA and log (I/T) with reciprocal of the absolute temperature are presented in Figures 8 (Arrhenius plot) and 9 (Transition state plot), respectively. Straight lines with coefficients of correlation (c. c) higher to 0.99 were obtained.

The E_a, ΔH_a and ΔS_a values were determined from the slopes of these plots. The calculated values of E_A, ΔH_a and ΔS_a in the absence and the presence of 10^{-3} M of DMA are given in table 5.

Table 5. The value of activation parameters E_a, ΔH_a and ΔS_a for steel in 0.5 M H_2SO_4 in the absence and presence of 10^{-3} M of DMA.

	E_a (kJ/mol)	ΔH_a (kJ/mol)	ΔS_a (J/mol)	E_a - ΔH_a (kJ/mol)
Blank	50.27	47.68	-77.92	2.59
DMA	43.44	40.85	-121.21	2.59

Inspection of these data reveals that the apparent activation energy E_a in 0.5 M H_2SO_4 solution in the absence of the DMA was 50.27 kJ/mol. The addition of DMA to the acid solution decreased the activation energy. Note that the reduction of the activation energy in the presence of DMA may be attributed to the chemisorption of the DMA inhibitor on C38 steel surface [27-28]. On the other hand, the inspection of the same table revealed that the thermodynamic parameters (ΔS_a and ΔH_a) for dissolution reaction of C38 steel in 0.5 M H_2SO_4 in the presence of inhibitor are lower than that obtained in the absence of inhibitor. The positive sign of ΔH_a reflects the endothermic nature of the C38 steel dissolution process suggesting that the dissolution of C38 steel is slow [29] in the presence of inhibitor. Large and negative value of entropies (ΔS_a) imply that the activated complex in the rate

determining step represents an association rather than a dissociation step [30], meaning that a decrease in disordering takes place on going from reactants to the activated complex [31-32].

4. CONCLUSIONS

2,10-dimethylacridin-9(10H)-one (DMA), has been found to inhibit the corrosion of C38 steel in 0.5M H_2SO_4 solution. Reasonably good agreement was observed between the data obtained from the weight-loss, electrochemical impedance spectroscopy and potentiodynamic polarization techniques. From the polarization measurements, it was found that the DMA behaved as a mixed-type inhibitor. This compound was found to inhibit the corrosion of C38 steel by adsorption on the metal surface. Adsorption of this inhibitor on C38 steel surface has been found to obey Langmuir's isotherm. The phenomenon of adsorption of DMA has been suggested to be chemical adsorption on the C38 steel electrode surface. The DMA inhibitor efficiency was temperature independent, and its addition led to decrease in the activation energy.

References

1. A. Anejjar, R. Salghi, A. Zarrouk, H. Zarrok, O. Benali, B. Hammouti, S. S. Al-Deyab, *Res Chem Intermed* DOI 10.1007/s11164-013-1244-7.(2013).
2. S. Merah, L. Larabi, O. Benali, Y. Harek, *Pig. Res. Tech*. 37(5) (2008) 291.
3. O. Benali, L. Larabi, Y. Harek, *J. App. Electrochem*. 39 (2009) 769.
4. D. Ben Hmamou, R. Salghi, A. Zarrouk, O. Benali, H. Zarrok, B. Hammouti, S. S. Al-Deyab, *Res. Chem. Intermed.*, DOI 10.1007/s11164-012-0892-3. (2012).
5. H. Zarrok, A. Zarrouk, R. Salghi, M. Assouag, B. Hammouti, H. Oudda, S. Boukhris, S. S. Al Deyab, I. Warad, *Der Pharmacia Lett.* 5 (2) (2013) 43.
6. A. H. Al Hamzi, H. Zarrok, A. Zarrouk, R. Salghi, B. Hammouti, S. S Al-Deyab, M. Bouachrine, A. Amine, F. Guenoun, *Int. J. Electrochem. Sci.* 8(2013) 2586 .
7. H. Oudda, A Zarrouk, R. Salghi, B. Hammouti, M. Ebn Touhami, S. S. Al-Deyab, H Zarrok, *GU. J. Sci.* 26(1) (2013) 21.
8. O. Benali, M. Ouazene, *Arab. J. Chem.* 4 (2011) 443.
9. H. Ouici, O. Benali, Y. Harek, L. Larabi, B. Hammouti, A. Guendouzi, *Res. Chem. Intermed.* 39 (2013) 2777.
10. D. Ben Hmamou, M.R. Aouad, R. Salghi, A. Zarrouk, M. Assouag, O. Benali, M . Messali, H. Zarrok, B. Hammouti, *J. Chem. Pharma. Res.* 4 (7) (2012) 3489.
11. D Ben Hmamou, M. R. Aouad, R Salghi, A. Zarrouk, M. Assouag, O. Benali, M. Messali, H. Zarrok, B. Hammouti, *J. Chem. Pharma. Res.* 4 (7) (2012) 3498.
12. L. Larabi, O. Benali, S. M. Mekelleche, Y. Harek, *Appl, Surf. Sci.* 253(2006) 1371.
13. M. R. Hamblin, T. Hasan, *Photochem. Photobiol. Sci.* 3(5) (2004) 436.
14. 14 J. W. Jonker, J. W Smit, R. F Brinkhuis, M. Maliepaard, J. H, Beijnen, J. H. M. Schellens, A. H. Schinkel, *Journal of the National Cancer Institute*. 2(20) (2000) 1651.
15. C. Das, *Indian Journal of Chemical Technology*. 3 (5) (1996) 259.
16. A. H. Al. Hamzi, H. Zarrok, A. Zarrouk, R. Salghi, B. Hammouti, M. Bouachrine, A. Amine, H. Oudda, *Der Pharmacia Lettre*. 5(2) (2013) 27.
17. A.Y Musa, A.A.H. Kadhum, A. B. Mohamad, M.S. Takriff, *Corros. Sci,* 52 (2010) 3331.
18. J. Zhang, X. L. Gong, H. H .Yu, M. Du, *Corros. Sci.* 53(2011)332.

19. Q. B. Zhang, Y. X Hua, *Acta*. 54 (2009) 1881.
20. E. H. McCafferty, N. Ackerman, *J. Electrochem. Soc.* 119 (1972)146.
21. F. Bentiss, M Traisnel, M. Lagrenée, *Corros. Sci.* 42 (2000)127.
22. S. Muralidharan, K. L .N. Phani, S. Pitchumani, S. Ravichhandran, S. V. K. Iyer, *J. Electrochem. Soc.* 142(1995)1478.
23. L. Larabi, Y. Harek, O Benali, S. Ghalem, *Prog. Org. Coat.* 54(2005) 256.
24. A. Dadgarinezhad, F Baghaei, *GU. J. Sci.* 24(2) *(*2011)219
25. V. R. Saliyan, A. V Adhikari, *Bull. Mater. Sci.* 31 (4) (2008)699.
26. A. H. Al Hamzi, H. Zarrok, A. Zarrouk, R. Salghi, B. Hammouti, M. Bouachrine, A.Amine, F. Guenoun, H. Oudda, *Der Pharma. Lett.* 5 (2) (2013) 27.
27. T. Szauer, A. Brandt, *Electrochim. Acta*. 26(1981)*1253*.
28. S. Sankarapapavinasam, F. Pushpanaden, M. F. Ahmed, *Corros. Sci.* 32(1991) 193.
29. N. M Guan, L. Xueming, L. Fei, *Mater. Chem. Phys.* 86 (2004) 59.
30. V. R Saliyan, A. V Adhikari, *Bull. Mater. Sci.* 31 (4) (2008) 699.
31. Marsh, J. *Advanced Organic Chemistry*" 3rd ed., Wiley Eastern New Delhi, 1988.
32. F. Bentiss, M. Lebrini, M. Lagrenee, *Corros. Sci.* 47(2005) 2915.